Loss of μ-crystallin causes PPARγ activation and obesity in high-fat diet-fed mice

Yohsuke Ohkubo[a †], Takashi Sekido[a †], Shin-ichi Nishio[a], Keiko Sekido[a], Junichiro Kitahara[a], Satoru Suzuki[b], Mitsuhisa Komatsu[a]

[a]Division of Diabetes, Endocrinology and Metabolism, Department of Internal Medicine, Shinshu University School of Medicine, Matsumoto 390-8621, Japan

[b]Department of Thyroid and Endocrinology, Division of Internal Medicine, School of Medicine, Fukushima Medical University Hospital, Fukushima, 960-1295, Japan

[†]Yohsuke Ohkubo and Takashi Sekido contributed equally to this work.

Correspondence to: Shin-ichi Nishio, M.D., Ph.D.

Division of Diabetes, Endocrinology and Metabolism, Department of Internal Medicine,

Shinshu University School of Medicine, 3-1-1 Asahi, Matsumoto, 390-8621 Japan

PHONE: +81-263-37-2686

FAX: +81-263-37-2710

e-mail: snishio@shinshu-u.ac.jp

Abstract

The thyroid hormone-binding protein μ-crystallin (CRYM) mediates thyroid hormone action by sequestering triiodothyronine in the cytoplasm and regulating the intracellular concentration of thyroid hormone. As thyroid hormone action is closely associated with glycolipid metabolism, it has been proposed that CRYM may contribute to this process by reserving or releasing triiodothyronine in the cytoplasm. We aimed to clarify the relationship between CRYM and glycolipid metabolism by comparing wild-type and CRYM knockout mice fed a high-fat diet. Each group was provided a high-fat diet for 10 weeks, and then their body weight and fasting blood glucose levels were measured. Although no difference in body weight was observed between the two groups with normal diet, the treatment with a high-fat diet was found to induce obesity in the knockout mice. The knockout group displayed increased dietary intake, white adipose tissue, fat cell hypertrophy, and hyperglycemia in the intraperitoneal glucose tolerance test. In CRYM knockout mice, liver fat deposits were more pronounced than in the control group. Enhanced levels of PPARγ, which is known to cause fatty liver, and ACC1, which is a target gene for thyroid hormone and is involved in the fat synthesis,

were also detected in the livers of CRYM knockout mice. These observations suggest that CRYM deficiency leads to obesity and lipogenesis, possibly in part through increasing the food intake of mice fed a high-fat diet.

Keywords: CRYM, high-fat diet, obesity, thyroid hormone

Abbreviations: thyroid hormone-binding protein μ-crystallin, CRYM; thyroid-Stimulating hormone, TSH; high-fat diet, HFD; white adipose tissue, WAT

INTRODUCTION

The prevalence of obesity is increasing worldwide, accompanied by elevated risks of additional metabolic diseases such as diabetes, hypertension, hyperlipidemia, and cardiovascular disease. It is caused by an imbalance between energy intake and expenditure [1]. Many hypotheses have been proposed concerning the mechanisms contributing to high-fat intake-related obesity, covering both genetic factors and metabolic processes [2, 3]. Thyroid hormone reportedly influences key metabolic pathways that control energy balance by regulating energy storage and expenditure [4]. It also activates both lipolysis and lipogenesis. However, as lipogenesis is primarily required to restore depleted fat stores, lipolysis typically predominates [5]. Moreover, thyroid hormone contributes to the conversion of preadipocytes to adipocytes [6]. Mu-crystallin (CRYM) is a cytosolic triiodothyronine (T3)-binding protein dependent on the presence of nicotinamide adenine dinucleotide phosphate [7, 8]. CRYM was first detected in the kangaroo lens and has since been found in the human brain, inner ear,

retina, kidney, heart, skeletal muscle, and adipose tissue [9]. It mediates thyroid hormone action through regulation of the intracellular T3 concentration [10]. CRYM knockout (KO) mice display normal growth and a normal heart rate; however, their serum concentrations of T3 and thyroxine (T4) are significantly reduced, despite not having any apparent alteration in the thyroid-stimulating hormone (TSH) content of their pituitary [11]. This indicates that the intracellular regulation of thyroid hormone activities is not exclusively performed by CRYM. CRYM expression increases and sustains the T3 responsiveness of genes in cells, especially in response to changes in the perinuclear T3 concentration [12]. This implies that CRYM may contribute to the regulation of thyroid hormone action in some circumstances where altered hormone levels do not appear warranted [12]. Serrano *et al.* reported that glucose tolerance deteriorates when CRYM expression decreases in human white adipose tissue (WAT) [13] and that CRYM acts as a metabolic regulator affecting glycolipid metabolism. CRYM is also believed to control muscle function through its regulation of thyroid hormone action. For example, uncoupling protein 3 has been found to be up-regulated in the muscle of CRYM KO mice [14].

Although it has already been established that thyroid hormone is involved in obesity induced by high fat diet (HFD), we hypothesized that CRYM may be involved in its onset. To clarify the roles of CRYM in glycolipid metabolism *in vivo*, we fed CRYM KO mice an HFD and assessed changes in their body weight, glucose tolerance, liver, and proportions of WAT.

Methods

Animal procedures

Male CRYM KO mice (*Crym* $^{-/-}$) bred on an SV/129 genetic background were used. As wild-type mice, SV/129 genetic background mice (*Crym* $^{+/+}$) were used with age-matched and no littermate controls. Wild-type mice as well. Mice were housed in a controlled environment (inverted 12-h daylight cycle, lights on at 9:00 am) with free access to food and water. The facility temperature was controlled to be constant at 23 ° C and 52% humidity. At eight weeks of age, the animals were switched to either a high-fat diet containing 60 % fat (HFD) (D12492, Research Diets, New Brunswick, USA) or a low-fat diet containing 10 % fat (LFD) (D12450B, Research Diets) for 10 weeks.

Body weight (BW) and fasting blood glucose were sampled at 17:00 after 8 hours of fasting per two weeks. Feeding amounts were measured by a specific multi feeder (Shinfactory, Fukuoka, Japan). All animal protocols were approved by the Shinshu University's animal ethics Committee (Approval No: 270002, Date: 2 Jun. 2017).

Glucose tolerance test

Following ten weeks of either LFD or HFD feeding, a glucose tolerance test (GTT) was performed by administering a 20 % glucose aqueous solution intraperitoneally at a dose of 2.0 g glucose/kg body weight after 4 hours of fasting. Blood samples were collected from the tail vein at 0, 15, 30, 60, 90, and 120 minutes post-injection. Blood glucose levels were measured using a Precision Pro monitoring system (Abbott Diabetes Care Inc., California, USA).

Insulin tolerance test

Following ten weeks of either LFD or HFD feeding, an insulin tolerance test (ITT) was performed by intraperitoneal injection with human insulin (Eli Lilly & Company, Indianapolis, USA) at a dose of 0.5 U insulin/kg body weight following a one-hour fast.

Blood samples were collected from the tail vein at 0, 30, 60, and 90 minutes post-injection. Blood glucose levels were measured using a Precision Pro monitoring system (Abbott Diabetes Care Inc.).

Histology

Tissue was fixed in 10 % buffered formalin, embedded in paraffin, sectioned at 6 μm, and stained with hematoxylin and eosin (HE). All images were acquired by AxioVision microscope (Zeiss, Oberkochen, Germany). For the evaluation of hepatic lipid depositions, we used the Vectra 3 imaging system (Perkin Elmer, Waltham, USA). Four visual fields from each of the three liver samples were analyzed from one animal for each group. Adipocyte size was measured using AxioVision microscope software (Zeiss) and Image J (Abramoff et al., 2004). One visual field, containing at least 50 cells, from each of four samples of epididymal white adipose tissue (eWAT) was analyzed from one animal for each group. The mean adipocyte size for each group was calculated.

Glucose-stimulated insulin secretion from islets *in vitro*

Primary islets from mice fed an HFD for 11 weeks were isolated by dissociating the

pancreas with collagenase (Type XI, Sigma-Aldrich, St. Louis, USA). The solution for isolation contained 1.5 mg/ml collagenase in 2.8 mM glucose Krebs-Ringer Bicarbonate (KRB) buffer composed of 120 mM NaCl, 4.8 mM KCl, 2.5 mM $CaCl_2$, 1.2 mM $MgCl_2$, and 24 mM $NaHCO_3$ with 0.2 % bovine serum albumin (Sigma-Aldrich). This solution was injected into the pancreatic duct. The inflated pancreas was removed and packed into a small plastic bag and shaken in 37 °C water for one minute, 100 times. Islets were picked out from the isolated solution. Five islets were plated per tube, and nine tubes were obtained from each mouse. Pre-incubations for all tubes were performed for 0.5 h in 2.8 mM glucose KRB buffer with 0.2 % bovine serum albumin. Following this, the islets were incubated for 1 h with 1 ml of KRB with 0.5% BSA at 2.8 mmol/l glucose, 16.7 mmol/l glucose, or 2.8 mmol/l glucose with 50 mmol/l KCl. The supernatants were then collected and stored at -20 °C. The insulin levels of the supernatants were determined using the Morinaga Ultra Sensitive Mouse/Rat Insulin ELISA Kit (Morinaga, Tokyo, Japan).

Quantitative reverse transcription PCR

Total tissue RNA was isolated using the RNeasy Protect mini kit (Qiagen). Quantitative

reverse transcription PCR was performed using the StepOnePlus Real-time PCR System (Thermofisher, Waltham, USA) with Fast SYBR Green Master Mix (TAKARA, Kusatsu, Japan). The primers used are listed in Sup. Table 1.

Statistical analysis

Data are presented as means ± SEM. All statistical analyses were carried out using PASW Statistics for Windows (v18.0, SPSS Inc.). Significant differences were determined by employing the Mann-Whitney U test. Differences with a p-value < 0.05 were considered statistically significant.

Results

CRYM KO mice fed an HFD display a significant increase in body and white adipose tissue weights

Over the course of ten weeks being fed an HFD, BW and fat areas on computed tomography iincreased significantly in the CRYM KO mice when compared to the wild-type mice (Figure 1A-C). However, no significant differences were seen in the BW of either genotype when fed the LFD. The daily food intake in the CRYM KO mice had

been higher than in the wild-type over every period studied (Figure 1D). The weight of eWAT and size of the adipocytes found in CRYM KO mice were significantly larger than those from wild-type mice (Figure 2A-C).

HFD induce no significant changes for glucose metabolism in CRYM KO mice

The fasting blood glucose levels of CRYM KO and wild-type mice were not significantly different when fed either the LFD (data not shown) or HFD (Figure 3A). GTT showed that the blood glucose level of HFD-fed CRYM KO mice was significantly higher than that of HFD-fed wild-type mice 60 minutes after glucose injection, but not at any other time point measured (Figure 3B).

After glucose injection, blood glucose tends to increase at HFD-fed CRYM KO mice (data not shown). There was no significantly difference about the insulin and glucose levels measured during the GTT and ITT respectively (Figure 3C and 3D). Glucose-stimulated insulin secretion from isolated islets was also similar between the two HFD groups (Figure 3E).

HFD-fed CRYM KO mice display prominent hepatic lipid depositions

Liver weight and triglyceride content followed an increasing trend in the HFD-fed CRYM KO group, but no significant differences were observed when compared to the HFD-fed wild-type mice (Figure 4A, B). However, the size of hepatic lipid depositions in CRYM KO mice appeared significantly larger than those seen in HFD-fed wild-type mice (Figure 4C, D).

Expression of PPAR γ in the CRYM KO group increased

To evaluate the potential effects of CRYM KO on liver inflammation and lipid metabolism following the HFD, we measured the expression of several genes involved in inflammation and lipogenesis. The inflammation-related gene tumor necrosis factor *(TNF) α* of HFD-fed CRYM KO on liver was significantly elevated when compared to the HFD-fed wild-type mice (Figure 4E), as was the lipogenesis-related gene Acetyl-CoA carboxylase (*Acc*) *1* (Figure 4G). Expression of peroxisome proliferator-activated receptor *(PPAR) γ* in the HFD-fed CRYM KO group increased by more than 10-fold relative to the HFD-fed wild-type group (Figure 4F).

No significant differences were detected for any gene that was assessed, including those related to appetite enhancement, such as those encoding the peptides neuropeptide Y (NPY) or pro-opiomelanocortin (POMC) (Sup. Figure 1).

DISCUSSION

Our findings indicate that loss of the thyroid hormone-binding protein CRYM causes obesity in mice fed an HFD. CRYM KO mice showed increased levels of adipose tissue and fat cell hypertrophy, decreased glucose tolerance, and increased inflammatory gene expression in their adipose tissue and liver following HFD feeding. Furthermore, *PPARγ* and *Acc1* expression levels were enhanced in the livers of HFD-fed CRYM KO mice when compared to wild-type. These data support that CRYM may be involved in lipogenesis and fat accumulation in the liver and may control energy balance.

Thyroid hormone is involved in the maintenance of body weight and energy expenditure [15]. Under excessive levels of thyroid hormone, energy production and lipolysis are accelerated while cholesterol levels are reduced. Thyroid hormone receptor (TR) alpha has been shown to increase in brown adipose tissue (BAT) with weight loss [16]. Conversely,

the expression of TR alpha and beta decrease in subcutaneous fat with weight gain [17]. Further, it has been reported that TSH is increased in obese patients [18] and decreased by weight loss [19]. Moreover, thyroid hormone may be involved in how prone or resistant a person may be to the development of obesity when consuming a high-fat diet [20, 21]. We observed that CRYM-deficient mice displayed increased WAT following an HFD. Both eWAT and retroperitoneal WAT, in addition to adipose cell area, were significantly increased in response to the combination of CRYM inactivation and HFD. T3 is known to stimulate local production of norepinephrine, thereby increasing lipolysis and reducing WAT [15]. Miao *et al.* have reported that liver X receptor (LXR) β activates TSH, resulting in a rise in thyroid hormone and subsequent increase in the activity of thyroid signaling in subcutaneous adipose tissue (SAT) [22]. LXRβ regulates T4 / T3 expression in SAT to regulate WAT amount, whereas deficiency of CRYM binding to T3 increases WAT amount; hence, it is possible that CRYM interacts with LXR in some way. We would like to investigate whether CRYM interacts with LXR by creating and analyzing double-knockout mice of LXRβ and CRYM.

Liver weight and triglyceride content tended to increase in CRYM KO mice fed an HFD, while the rate of lipid deposition increased significantly and the expression of PPARγ was markedly enhanced. Increased PPARγ expression reportedly leads to a steatotic liver [23]. PPARγ activates genes involved in lipogenesis [24, 25]. Hepatocyte- and macrophage-specific knockout of PPARγ protects mice against diet-induced hepatic steatosis [26]. Although it remains unclear how CRYM and PPARγ expression may be related, it is apparent that when CRYM is deficient, PPARγ expression is remarkably enhanced and correlates with the onset of hepatic steatosis.

On the other hand, thyroid hormone induces *de novo* lipogenesis via transcription of several key lipogenic genes such as *Acc1* and fatty acid synthase *(Fasn)*. Indirect regulation of hepatic lipogenesis occurs through the activation of additional transcription factors such as sterol regulatory element-binding protein 1C (SREBP1C), LXRs, and carbohydrate-responsive element-binding protein (ChREBP) [27]. Our results indicate that when CRYM was inactivated in an HFD environment, *Acc1* expression was significantly increased while *Fasn* and *Sreb1c* followed a non-significant trend towards increased expression, as compared to HFD-fed wild-type

mice. Interestingly, *Acc1*, *Fasn*, and *Sreb1c* have already been shown to either increase significantly or show a tendency towards increasing in HFD-fed, obesity-prone mice [28]. ACC1 is enriched in the liver and is regulated by TR at the transcriptional level through the ACC1 promoter II [29]. ACC1 is a key enzyme that catalyzes the ATP-dependent carboxylation of acetyl -CoA to malonyl- CoA and controls fatty acid metabolism. Endo *et al.* demonstrated that ACC1 plays a crucial role in the appropriate function of retinoic-acid-receptorrelated orphan receptor (ROR) through fatty acid synthesis and regulates the obesity-related pathology of helper T cells [30]. They also showed a strong correlation between IL-17A-producing CD45RO (+) CD4 T cells and the expression of ACC1 in obese subjects. These data suggest that CRYM may restrict the expression of these genes in the presence of T3.

We also analyzed the glucose metabolism of HFD-fed CRYM KO mice using an intraperitoneal GTT. Blood glucose levels of CRYM KO mice were significantly higher than those of mice from the wild-type group at 1 hour after the challenge. However, no differences were seen in the insulin resistance, plasma insulin concentration, fasting blood glucose, or insulin secretion from isolated islets between the two groups. Serrano

et al. have shown that CRYM overexpression leads to increased levels of phosphorylated Akt, a crucial component of the insulin signaling pathway [13]. Paired with the fact that CRYM appears to affect the expression of ACC1, we believe it is likely involved in glucose metabolism. While there was no difference in the systemic insulin resistance between the two HFD groups, it is possible that insulin resistance was induced in the liver alone, in response to hepatic steatosis, which may have contributed to hyperglycemia after glucose injection.

López *et al.* reported that thyroid hormone promotes thermogenesis not only through actions on peripheral muscles, but also through the BAT, hypothalamus, and pituitary gland, comprising the hypothalamic–pituitary–thyroid (HPT) axis [31]. Thyrotropin-releasing hormone (TRH) exists in the hypothalamus and controls TSH. Cocaine-amphetamine-regulated transcript (CART) stimulates TRH synthesis and release while NPY inhibits TRH transcription [32]. As we saw a higher food intake in the CRYM KO group than the wild-type when supplied with the HFD, we suggest that CRYM is involved in the HPT axis. However, as no significant differences were detected between the HFD CRYM KO and wild-type groups for genes encoding appetite enhancing

peptides such as NPY and POMC (Sup. Figure 1). A more detailed analysis is required to identify the mechanisms by which CRYM acts along this axis. However, it is very unlikely that the onset of hepatic steatosis and the remarkable increase seen in PPARγ expression in CRYM KO mice fed an HFD can be explained solely as the effects of an increased appetite.

In summary, CRYM appears to suppress the activation of lipogenesis in the liver. When mice are fed an HFD in the absence of CRYM, the target genes PPARγ and T3 are activated, resulting in obesity and a fatty liver. Based on our data, we propose that CRYM has an essential role in the protection against fatty liver and obesity when dietary fat intake is high.

Acknowledgments

The authors thank Dr. Toru Aizawa for their invaluable comments.

We would like to thank Editage (*www.editage.jp*) for English language editing.

Author Contributions

Y.O. and T.S. performed the research and wrote the manuscript. S.N. designed and performed the research and wrote the manuscript. J.K. and K.S. contributed to the data analysis. S.S. and M.K. reviewed and edited the manuscript.

Funding

This work was supported by the JSPS KAKENHI (grant number 16K09799).

Disclosure Statement

Mitsuhisa Komatsu has received honoraria for lectures from Novo Nordisk, Sanofi, Eli Lilly, Kissei Pharmaceutical Co. Ltd., MSD, Takeda Pharmaceutical Co. Ltd., Ono Pharmaceutical Co. Ltd., and Sumitomo Dainippon Pharma Co. Ltd.

REFERENCES

[1] P. Bjorntorp, Obesity, Lancet, 350 (1997) 423-426.

[2] S. Chang, B. Graham, F. Yakubu, D. Lin, J.C. Peters, J.O. Hill, Metabolic differences between obesity-prone and obesity-resistant rats, Am. J. Physiol. 259 (1990) R1103–1110.

[3] B.E. Levin, S. Hogan, A.C. Sullivan, Initiation and perpetuation of obesity and obesity resistance in rats, Am. J. Physiol. 256 (1989) R766–771.

[4] S.Y. Cheng, J.L. Leonard, P.J. Davis, Molecular aspects of thyroid hormone actions, Endocr. Rev. 31 (2010) 139–170.

[5] J.H. Oppenheimer, H.L. Schwartz, J.T. Lane, M.P. Thompson, Functional relationship of thyroid hormone-induced lipogenesis, lipolysis, and thermogenesis in the rat, J. Clin. Invest. 87 (1991) 125–132.

[6] M.J. Obregon, Thyroid hormone and adipocyte differentiation, Thyroid 18 (2008) 185–195.

[7] A. Beslin, M.P. Vie, J.P. Blondeau, J. Francon, Identification by photoaffinity labelling of a pyridine nucleotide-dependent tri-iodothyronine-binding protein in the cytosol of cultured astroglial cells, Biochem. J. 305 (Pt 3) (1995) 729–737.

[8] K. Hashizume, M. Kobayashi, T. Miyamoto, Active and inactive forms of 3,5,3'-triiodo-L-thyronine (T3)-binding protein in rat kidney cytosol: possible role of nicotinamide adenine dinucleotide phosphate in activation of T3 binding, Endocrinology 119 (1986) 710–719.

[9] R.Y. Kim, R. Gasser, G.J. Wistow, mu-crystallin is a mammalian homologue of Agrobacterium ornithine cyclodeaminase and is expressed in human retina, Proc. Natl. Acad. Sci. U. S. A. 89 (1992) 9292–9296.

[10] S. Suzuki, J. Mori, K. Hashizume, mu-crystallin, a NADPH-dependent T(3)-binding protein in cytosol, Trends Endocrinol. Metab. 18 (2007) 286–289.

[11] S. Suzuki, N. Suzuki, J. Mori, A. Oshima, S. Usami, K. Hashizume, micro-Crystallin as an intracellular 3,5,3'-triiodothyronine holder in vivo, Mol. Endocrinol. 21 (2007) 885–894.

[12] K. Takeshige, T. Sekido, J. Kitahara, Y. Ohkubo, D. Hiwatashi, H. Ishii, S. Nishio, T. Takeda, M. Komatsu, S. Suzuki, Cytosolic T3-binding protein modulates dynamic alteration of T3-mediated gene expression in cells, Endocr. J. 61 (2014) 561–570.

[13] M. Serrano, M. Moreno, F.J. Ortega, G. Xifra, W. Ricart, J.M. Moreno-Navarrete, J.M. Fernandez-Real, Adipose tissue mu-crystallin is a thyroid hormone-binding protein associated with systemic insulin sensitivity, J. Clin. Endocrinol. Metab. 99 (2014) E2259–2268.

[14] D. Seko, S. Ogawa, T.S. Li, A. Taimura, Y. Ono, mu-Crystallin controls muscle function through thyroid hormone action, Faseb J. 30 (2016) 1733–1740.

[15] R. Mullur, Y.Y. Liu, G.A. Brent, Thyroid hormone regulation of metabolism, Physiol. Rev. 94 (2014) 355–382.

[16] M. Nannipieri, F. Cecchetti, M. Anselmino, S. Camastra, P. Niccolini, M. Lamacchia, M. Rossi, G. Iervasi, E. Ferrannini, Expression of thyrotropin and thyroid hormone receptors in adipose tissue of patients with morbid obesity and/or type 2 diabetes: effects of weight loss, Int. J. Obes. (Lond), 33 (2009) 1001–1006.

45 [17] C. Bairras, A. Redonnet, H. Dabadie, H. Gin, C. Atgie, V. Pallet, P. Higueret, C.
46 Noel-Suberville, RARgamma and TRbeta expressions are decreased in PBMC and
47 SWAT of obese subjects in weight gain, J. Physiol. Biochem. 66 (2010) 29–37.
48 [18] A. Nyrnes, R. Jorde, J. Sundsfjord, Serum TSH is positively associated with BMI,
49 Int. J. Obes. (Lond), 30 (2006) 100–105.
50 [19] T. Reinehr, A. Isa, G. de Sousa, R. Dieffenbach, W. Andler, Thyroid hormones and
51 their relation to weight status, Horm. Res. 70 (2008) 51–57.
52 [20] R.L. Araujo, B.M. de Andrade, A.S. de Figueiredo, M.L. da Silva, M.P. Marassi, S.
53 Pereira Vdos, E. Bouskela, D.P. Carvalho, Low replacement doses of thyroxine during
54 food restriction restores type 1 deiodinase activity in rats and promotes body protein
55 loss, J. Endocrinol. 198 (2008) 119–125.
56 [21] A.C. Bianco, Minireview: cracking the metabolic code for thyroid hormone
57 signaling, Endocrinology 152 (2011) 3306–3311.
58 [22] Y. Miao, W. Wu, Y. Dai, L. Maneix, B. Huang, M. Warner, J.A. Gustafsson, Liver
59 X receptor beta controls thyroid hormone feedback in the brain and regulates browning

of subcutaneous white adipose tissue, Proc. Natl. Acad. Sci. U. S. A. 112 (2015) 14006–14011.

[23] A.K.S. Silva, C.A. Peixoto, Role of peroxisome proliferator-activated receptors in non-alcoholic fatty liver disease inflammation, Cell. Mol. Life Sci. 75 (2018) 2951–2961.

[24] S. Yu, K. Matsusue, P. Kashireddy, W.Q. Cao, V. Yeldandi, A.V. Yeldandi, M.S. Rao, F.J. Gonzalez, J.K. Reddy, Adipocyte-specific gene expression and adipogenic steatosis in the mouse liver due to peroxisome proliferator-activated receptor gamma1 (PPARgamma1) overexpression, J. Biol. Chem. 278 (2003) 498–505.

[25] O. Gavrilova, M. Haluzik, K. Matsusue, J.J. Cutson, L. Johnson, K.R. Dietz, C.J. Nicol, C. Vinson, F.J. Gonzalez, M.L. Reitman, Liver peroxisome proliferator-activated receptor gamma contributes to hepatic steatosis, triglyceride clearance, and regulation of body fat mass, J. Biol. Chem. 278 (2003) 34268–34276.

[26] E. Moran-Salvador, M. Lopez-Parra, V. Garcia-Alonso, E. Titos, M. Martinez-Clemente, A. Gonzalez-Periz, C. Lopez-Vicario, Y. Barak, V. Arroyo, J. Claria, Role for

75 PPARgamma in obesity-induced hepatic steatosis as determined by hepatocyte- and
76 macrophage-specific conditional knockouts, Faseb J. 25 (2011) 2538–2550.
77 [27] Y.Y. Liu, G.A. Brent, Thyroid hormone crosstalk with nuclear receptor signaling in
78 metabolic regulation, Trends Endocrinol. Metab. 21 (2010) 166–173.
79 [28] S.F. Xia, X.M. Duan, L.Y. Hao, L.T. Li, X.R. Cheng, Z.X. Xie, Y. Qiao, L.R. Li, X.
80 Tang, Y.H. Shi, G.W. Le, Role of thyroid hormone homeostasis in obesity-prone and
81 obesity-resistant mice fed a high-fat diet, Metabolism 64 (2015) 566–579.
82 [29] C. Huang, H.C. Freake, Thyroid hormone regulates the acetyl-CoA carboxylase PI
83 promoter, Biochem. Biophys. Res. Commun. 249 (1998) 704–708.
84 [30] Y. Endo, H.K. Asou, N. Matsugae, K. Hirahara, K. Shinoda, D.J. Tumes, H.
85 Tokuyama, K. Yokote, T. Nakayama, Obesity Drives Th17 Cell Differentiation by
86 Inducing the Lipid Metabolic Kinase, ACC1, Cell Rep. 12 (2015) 1042–1055.
87 [31] M. Lopez, L. Varela, M.J. Vazquez, S. Rodriguez-Cuenca, C.R. Gonzalez, V.R.
88 Velagapudi, D.A. Morgan, E. Schoenmakers, K. Agassandian, R. Lage, P.B. Martinez de
89 Morentin, S. Tovar, R. Nogueiras, D. Carling, C. Lelliott, R. Gallego, M. Oresic, K.
90 Chatterjee, A.K. Saha, K. Rahmouni, C. Dieguez, A. Vidal-Puig, Hypothalamic AMPK

and fatty acid metabolism mediate thyroid regulation of energy balance, Nat. Med., 16 (2010) 1001–1008.

[32] M.I. Chiamolera, F.E. Wondisford, Minireview: Thyrotropin-releasing hormone and the thyroid hormone feedback mechanism, Endocrinology 150 (2009) 1091–1096.

Figure legends

Figure 1

Gross body and feed parameters for CRYM KO and wild-type mice fed an HFD or LFD. A) Body weights of HFD mice (n = 25 for wild-type and CRYM KO each) and LFD mice (n = 8 for wild-type, n = 6 for CRYM KO). Over the course of ten weeks being fed an HFD, BW increased significantly in the CRYM KO mice. B) Representative photographs and C) Representative abdominal computer-tomography images of wild-type and CRYM KO mice. D) HFD feed amount per mouse over 10 weeks (n = 7 for wild-type and CRYM KO each). The rates of food intake (mg/g BW

106 per day) were higher for the CRYM KO mice than for the wild-type over every period

107 studied.

108 Figure 2

109 Adipose tissue and adipocyte analyses.

110 A) White adipose tissue weights (n = 7 for wild-type, n = 6 for CRYM KO). Both

111 epididymal WAT and retroperitoneal WAT were significantly increased in CRYM KO

112 mice fed an HFD. B) Representative images of epididymal white adipose tissues

113 (eWAT) as visualized with hematoxylin and eosin. C) Adipocyte size as calculated from

114 eWAT sections (n = 4 for wild-type and CRYM KO each). The size of the adipocytes

115 found in CRYM KO mice were significantly larger than those from wild-type mice.

116

117 Figure 3

118 Impaired glucose tolerance in CRYM KO mice fed an HFD. A) Fasting blood glucose

119 levels in HFD mice (n = 26 for wild-type and CRYM KO each). B) Blood glucose

120 levels during the GTT following 10 weeks feeding on the HFD (n = 7 for wild-type and

121 n = 6 for CRYM KO).

C) serum insulin levels during the GTT following 10 weeks feeding on the HFD (n = 7 for wild-type and n = 6 for CRYM KO). D) Blood glucose levels during the ITT after 10 weeks feeding on the HFD (n = 9 for wild-type and n = 10 for CRYM KO). E) Insulin levels measured in the supernatant of isolated primary islets from mice following 11 weeks feeding on the HFD (n = 9 for wild-type and CRYM KO each).

Figure 4

Altered liver characteristics in CRYM KO mice after HFD feeding. A) Liver weights and B) triglyceride content in HFD mice (n = 7 for wild-type and n = 6 for CRYM KO). C) Lipid deposition rate (n = 3 for wild-type and CRYM KO each). D) Representative liver pathology as visualized with hematoxylin and eosin. E) mRNA analysis of inflammatory genes. *TNFα* of HFD-fed CRYM KO was significantly elevated. F) mRNA analysis of PPARs genes. *PPARγ* in the HFD-fed CRYM KO increased relative to the HFD-fed wild-type group. G) mRNA analysis of thyroid hormone target genes. *Acc1* was significantly elevated.

Supplementary Figure 1. The expression levels of mRNA related appetite in the brains of HFD mice (n = 7 for wild-type and n = 6 for CRYM KO). AgRP (agouti-related peptide), NPY, POMC and SOCS-3 (suppressor of cytokine signaling-3).

Supplementary table 1. Primers used for quantitative reverse transcription PCR.

Figure 1

A

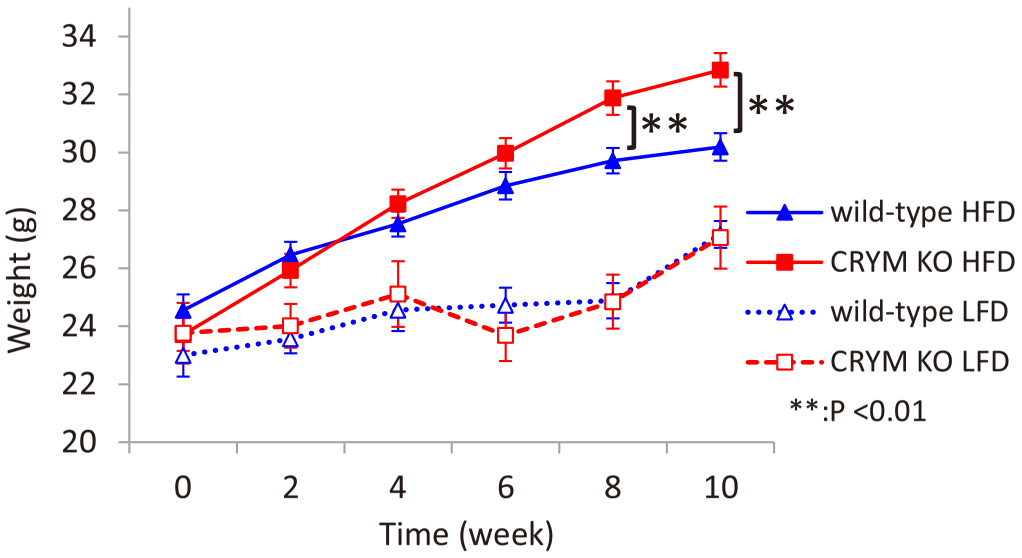

B

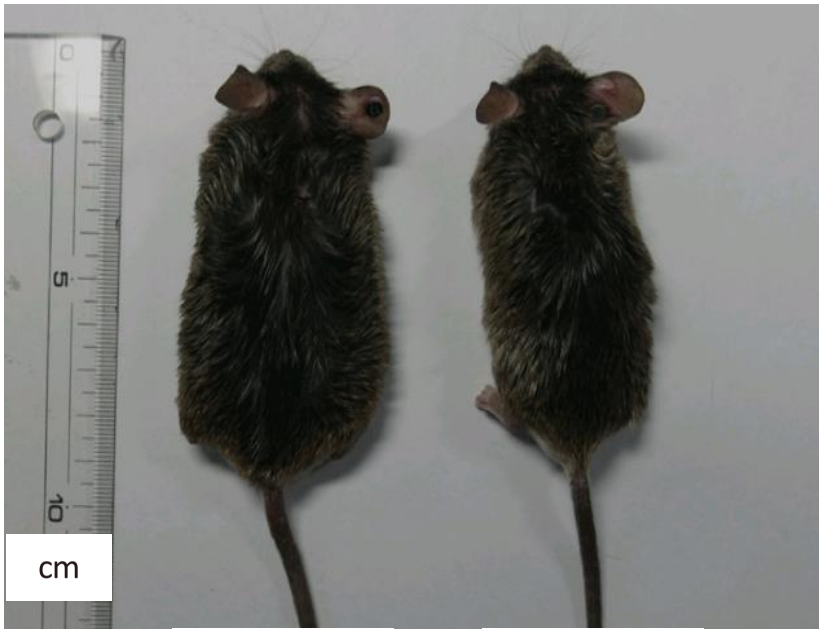

C

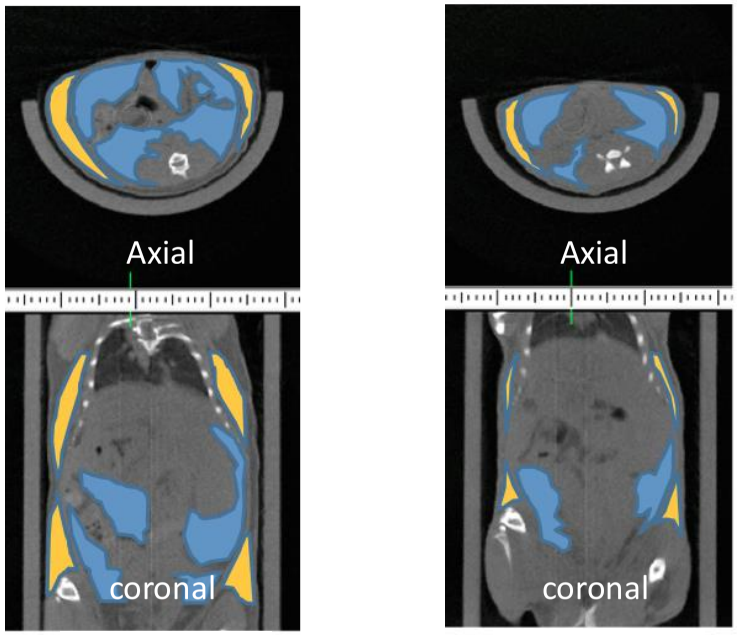

D

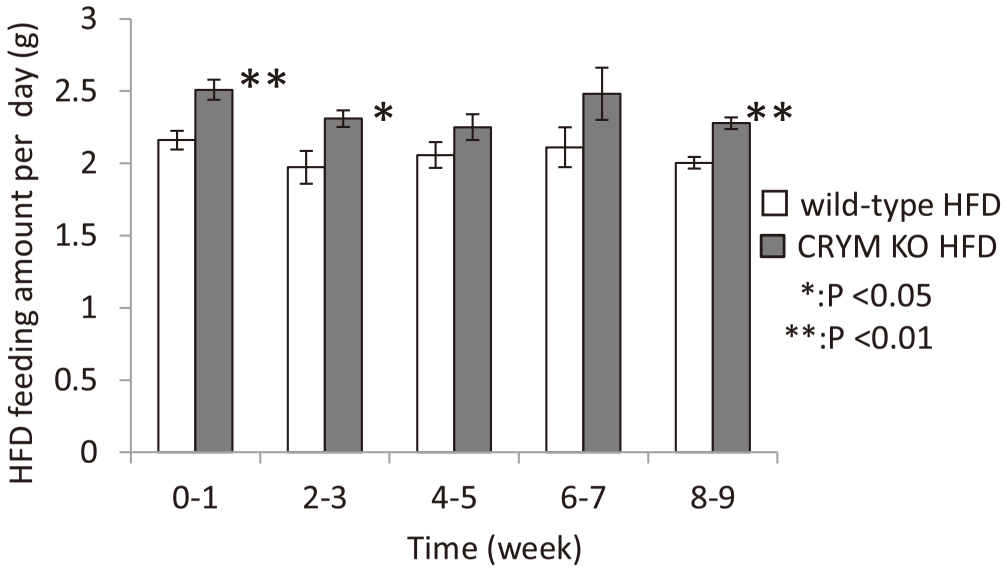

Ohkubo and Sekido *et.al*

Figure 2

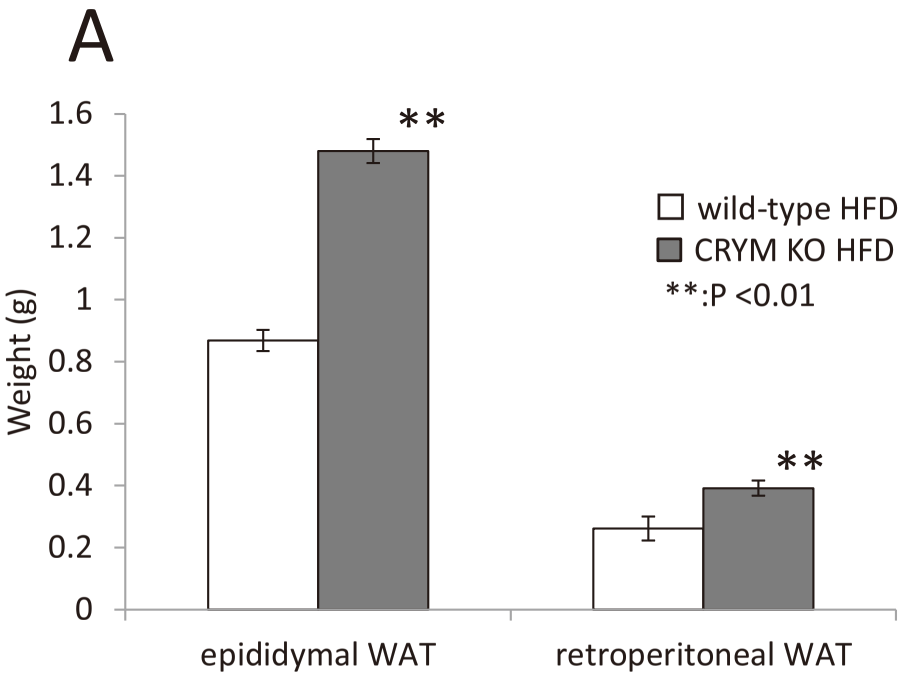

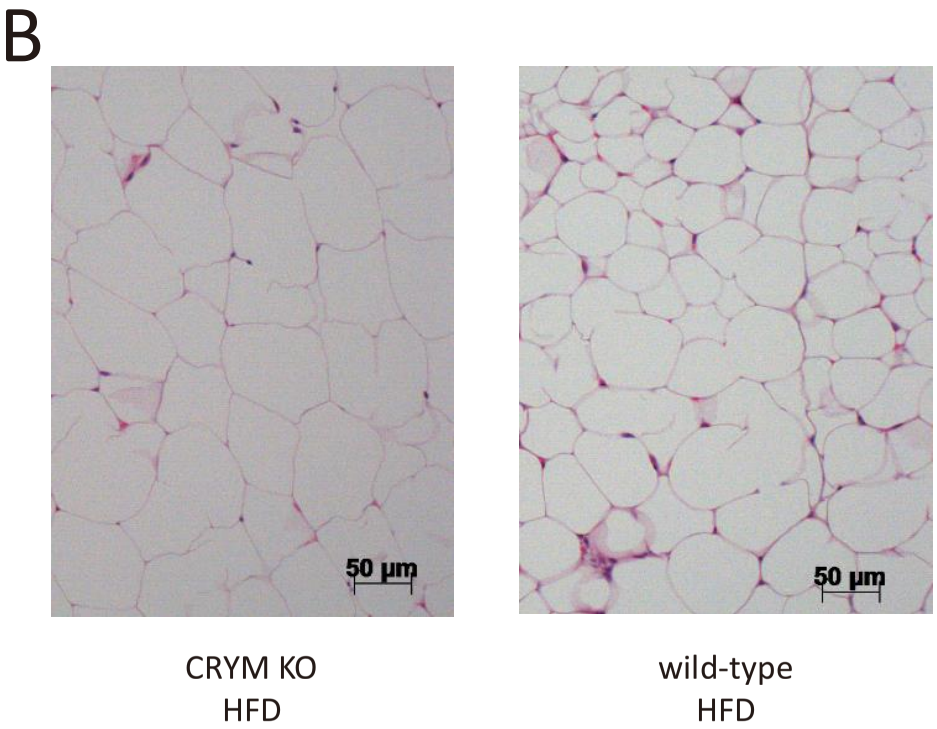

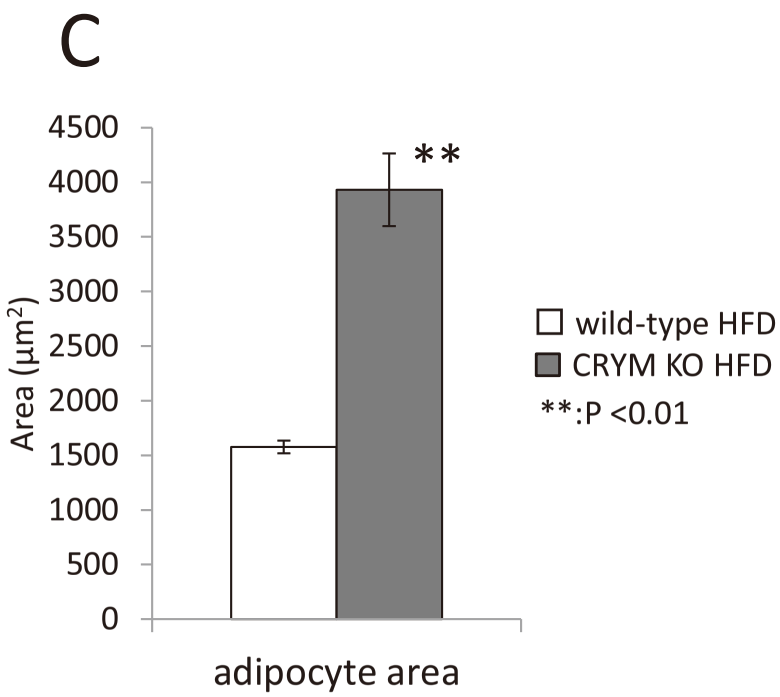

Ohkubo and Sekido *et.al*

Figure 3

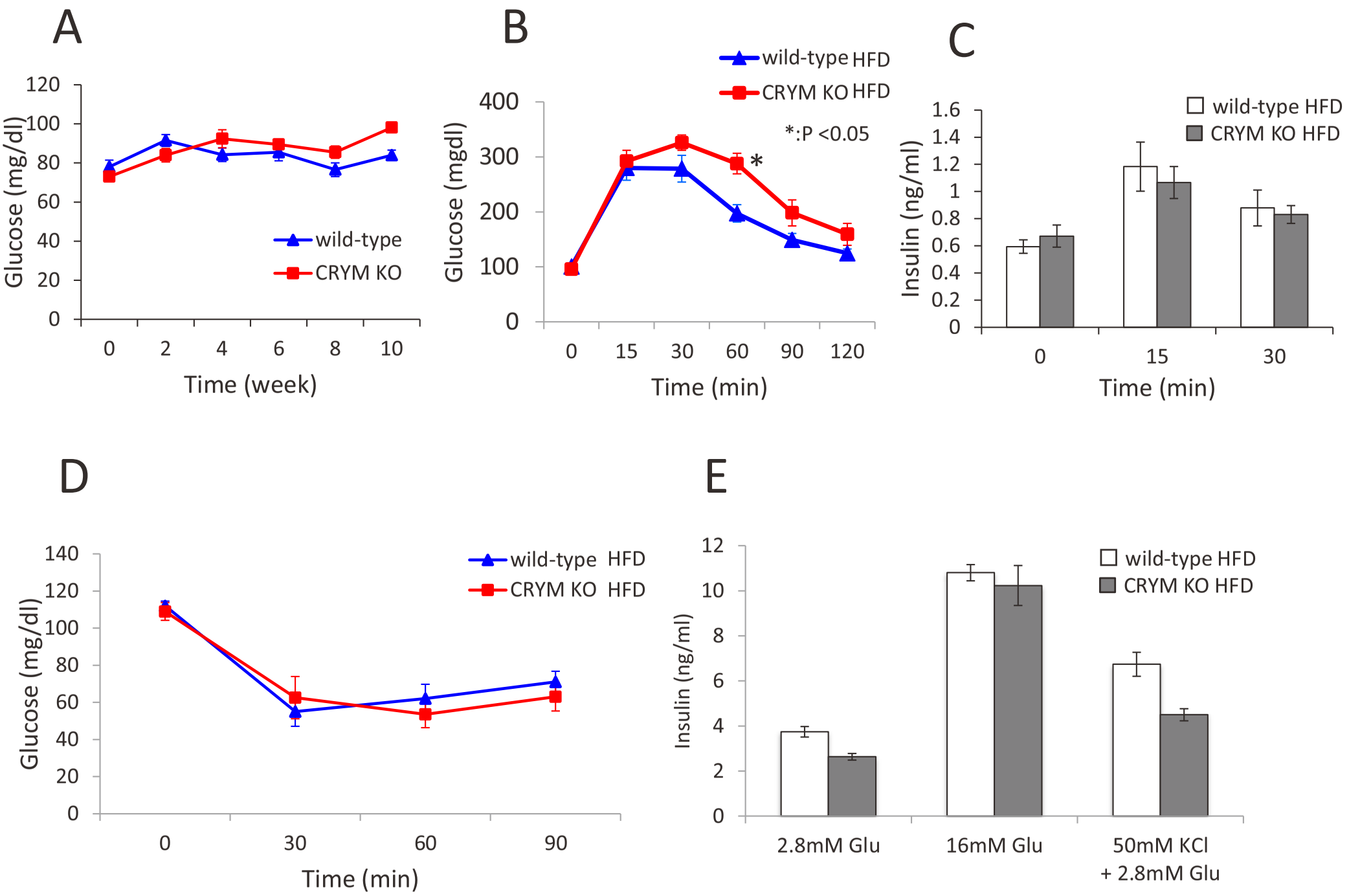

Ohkubo and Sekido *et.al*

Figure 4

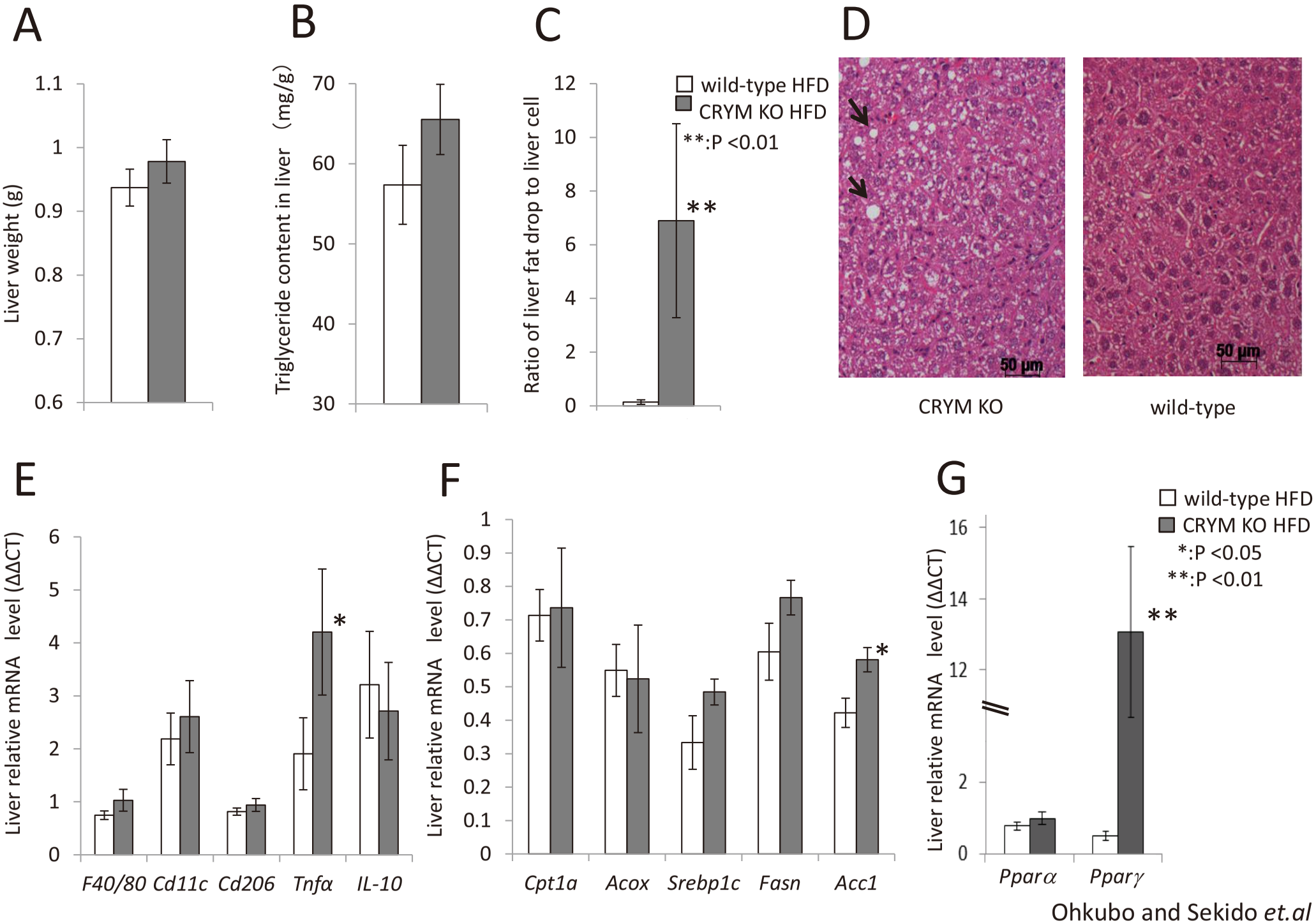

Ohkubo and Sekido *et.al*

Supplemental figure 1

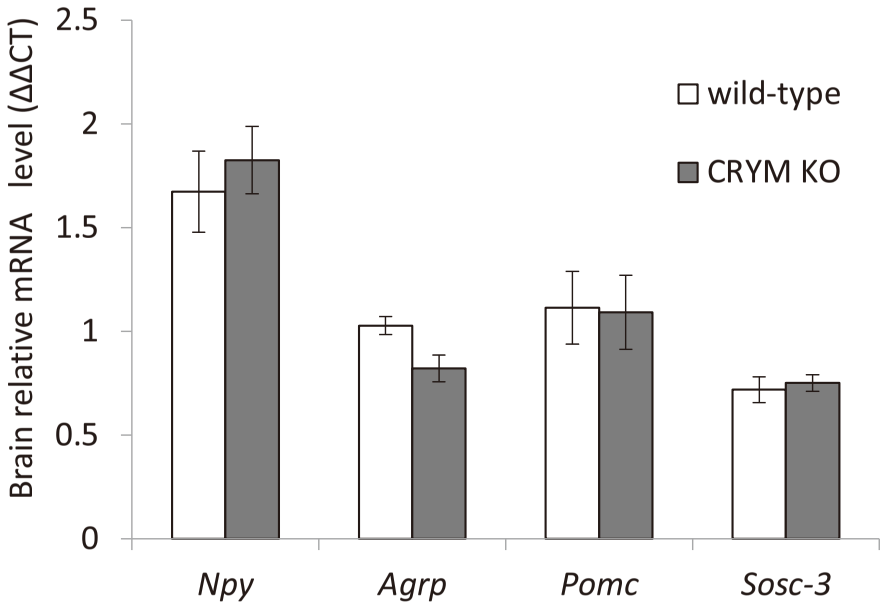

Supplementary Figure 1.
The expression levels of mRNA related appetite in the brains of HFD mice (n = 7 for wild-type and n = 6 for CRYM KO). The mRNAs are AgRP (agouti-related peptide), NPY (neuropeptide Y), POMC (pro-opiomelanocortin) and SOCS-3 (suppressor of cytokine signaling-3).

Supplemental table 1

Primers used for quantitative reverse transcription PCR

Gene	Foward Sequence(5'-3')	Reverse Sequence(5'-3')
Crym	ATGCGCTCACCACCAAGTTA	ATTTCCATCCATGACCGCCA
Pparα	AGGCTGTAAGGGCTTCTTTCG	GGCATTTGTTCCGGTTCTTC
Pparϒ2	GCATGGTGCCTTCGCTGA	TGGCATCTCTGAGTCAACCATG
Cd11c	GCCATTGAGGGCACAGAGA	GAAGCCCTCCTGGGACATCT
Srebp1c	CGGAAGCTGTCGGGGTAG	GTTGTTGATGAGCTGGAGCA
Fasn	CCTGGATAGCATTCCGAACCT	AGCACATCTCGAAGGCTACACA
Acc1	TGAGATTGGCATGGTAGCCTG	CTCGGCCATCTGGATATTCAG
Acox	GCCTTTGTTGTCCCTATCCGT	CGATATCCCCAACAGTGATGC
Cpt1a	CCTGCATTCCTTCCCATTTG	TGCCCATGTCCTTGTAATGTG
Cd206	CGGTGAACCAAATAATTACCAAAAT	GTGGAGCAGGTGTGGGCT
Pck1	CCACAGCTGCTGCAGAACA	GAAGGGTCGCATGGCAAA
F4/80	CTTTGGCTATGGGCTTCCAGTC	GCAAGGAGGACAGAGTTTATCGTG
Cd11c	GCCATTGAGGGCACAGAGA	GAAGCCCTCCTGGGACATCT
Tnfα	ACCCTCACACTCAGATCATCTTC	TGGTGGTTTGCTACGACGT
IL10	GCGCTGTCATCGATTTCTCC	CACCTGCTCCACTGCCTTG
Ucp1	CACCTTCCCGCTGGACACT	CCCTAGGACACCTTTATACCTAATGG
Npy	CTCCGCTCTGCGACACTAC	AATCAGTGTCTCAGGGCT
Agrp	GCGGAGGTGCTAGATCCA	AGGACTCGTGCAGCCTTA
Pomc	ACCTCACCACGGAGAGCA	GCGAGAGGTCGAGTTTGC
Socs-3	GCGGGCACCTTTCTTATCC	TCCCCGACTGGGTCTTGAC

Ohkubo and Sekido *et.al*